One-shot NMR analysis of microbial secretions identifies highly potent proteasome inhibitor

Stein, M L ; Beck, P ; Kaiser, M ; Dudler, R ; Becker, C F W ; Groll, M

Abstract: Natural products represent valuable lead structures for drug discovery. However, for most bioactive compounds no cellular target is yet identified and many substances predicted from genome analysis are inaccessible due to their life stage-dependent biosynthesis, which is not reflected in common isolation procedures. In response to these issues, an NMR-based and target-directed protease assay for inhibitor detection of the proteasome was developed. The methodology is suitable for one-shot identification of inhibitors in conglomerates and crude culture broths. The technique was applied for analysis of the different life stages of the bacterium Photorhabdus luminescens, which resulted in the isolation and characterization of cepafungin I (CepI), the strongest proteasome inhibitor described to date. Its biosynthesis is strictly regulated and solely induced by the specific environmental conditions determined by our methodology. The transferability of the developed technique to other drug targets may disclose an abundance of novel compounds applicable for drug development.

DOI: https://doi.org/10.1073/pnas.1211423109

One-shot NMR analysis of microbial secretions identifies highly potent proteasome inhibitor

Martin Stein[1], Philipp Beck[1], Markus Kaiser[2], Robert Dudler[3], Christian F. W. Becker[4] and Michael Groll[1,5]

[1]Center for Integrated Protein Science at the Department Chemie, Lehrstuhl für Biochemie, Technische Unversität München, Lichtenbergstraße 4, 85748 Garching, Germany.

[2]Center for Medical Biotechnology at the Department of Biology, Universität Duisburg-Essen, Universitätsstraße 2, 45141 Essen, Germany.

[3]Zurich-Basel Plant Science Center, Institute of Plant Biology, University of Zurich, Zollikerstraße 107, 8008 Zurich, Switzerland.

[4]Institut für Biologische Chemie, Universität Wien, Währinger Straße 38, 1090 Wien, Austria.

[5]Correspondence to michael.groll@ch.tum.de, phone: 0049-89-28913361

Major Classification: Physical Sciences (Chemistry)

Minor Classification: Biological Sciences (Biochemistry)

Natural products represent valuable lead structures for drug discovery. However, for most bioactive compounds no cellular target is yet identified and many substances predicted from genome analysis are inaccessible due to their life-stage dependent biosynthesis, which is not reflected in common isolation procedures. In response to these issues an NMR based and target directed protease assay for inhibitor detection of the proteasome was developed. The methodology is suitable for one-shot identification of inhibitors in conglomerates and culture broths. The technique was applied for analysis of the different life-stages of the bacterium *P. luminescens*, which resulted in the isolation and characterization of cepafungin I (CepI), the strongest proteasome inhibitor described to date. Its biosynthesis is strictly regulated and solely induced by the specific environmental conditions determined by our methodology. The transferability of the developed technique to other drug targets may disclose an abundance of novel compounds applicable for drug development.

The eukaryotic proteasome core particle (CP) is a 720 kDa multicatalytic protein degradation machinery and constitutes the main non-lysosomal protein degradation system in cells (1, 2). Its structure is composed of four stacked heptameric rings which contain the active subunits β1, β2 and β5 with an electrophilic Thr-1O$^{\gamma}$ at their N-termini (3-5). They exhibit the proteolytic activities denominated caspase-like (CL), trypsin-like (TL) and chymotrypsin-like (ChTL) according to the chemical nature of their specificity pockets (6). Being involved in many cellular processes such as cell proliferation and antigen presentation, the CP is a potential target for the treatment of diseases as diverse as cancer or autoimmunity (7). The blockbuster drug Velcade, a synthetic dipeptide boronic acid, was the first proteasome inhibitor approved for cancer therapy (8). However, because of its severe side effects (9) and the vast potential of proteasome inhibitors with regard to other diseases (7), there is a high demand for the development of novel agents. Lead structures for new drugs are often deduced

from natural compounds, as they are evolutionary optimized (10). A current and highly prominent example is Carfilzomib, a proteasome inhibitor in clinical phase III trials (11), which was derived from the natural product inhibitor epoxomicin (12, 13). Although other natural compounds have been elucidated in past decades (10), a persistent challenge for the identification of potent proteasome inhibitors still remains. However, in our days natural product research suffers generally from two major limitations. First, for most compounds described in literature, no cellular target has been identified so far. In general, this complicates the rational application of bioactive compounds. Second, the life-stage dependent metabolite pattern of many organisms is not reflected by commonly applied growth conditions, thus leading to a severely limited accessibility within the huge spectrum of natural substances.

Results

Development of an NMR based proteasome assay. Addressing both issues, we have developed a novel proteasome assay for screening of inhibitor secretion under various growth conditions. It uses a peptide substrate of the CP, which was atom-selectively labeled for NMR spectroscopy and derived from the digestion pattern of the murine JAK1 tyrosine kinase, a well characterized natural substrate of the 20S proteasome (14). The peptide sequence is adapted towards specificity for the ChTL activity as inhibitors against the corresponding β5 subunit exert high cytotoxicity and strongly influence adaptive immune response by MHCI presentation. By introducing a carbonyl ^{13}C probe at the scissile bond, hydrolysis can be qualitatively and quantitatively evaluated by a peak shift in the ^{13}C-NMR spectrum from 173 to 177 ppm, corresponding to the amide educt and the carboxylic acid product, respectively (Fig. 1). Synthesis of the substrate was achieved by standard Boc-based solid phase peptide chemistry, whereas the peptide cleavage site was determined by LC-MS analysis of the digestion products in an *in vitro* assay. Confirming the specificity of the probe molecule towards the β5 subunit, the hydrolysis was prevented in the same assay after addition of the

synthetic boronic acid inhibitor MG262 (15), which exhibits inhibition merely of the ChTL activity.

The assay displays the superiority of NMR techniques over common UV-Vis and fluorescence based methods by overcoming color quenching artifacts, which produce a plentitude of false positive or negative results in high-throughput arrays. In contrast, the developed approach yields unambiguous readout information and is applicable to extremely heterogeneous and colored conglomerates present, for example, in culture media. The technique is suitable for high-throughput analysis, as the recording time in a standard 500 MHz NMR machine, equipped with an autosampler, is only about 15 minutes per assay. Thus, a typical sample number of 96 experiments can be processed within one day. With a volume of approximately 500 µl, the methodology allows to screen a large number of small cultures at different growth conditions in short periods.

Application of the technique in a real-case scenario. For evaluation of the NMR assay by a positive control, we analyzed secretions of *Pseudomonas syringae*, which causes the brown spot disease in common bean plants and whose virulence is decisively determined by the proteasome inhibitor syringolin A (SylA), a member of the syrbactin family. The bacteria were grown in SRM_{AF} medium, which contains the phenolic sugar arbutin present in plant leaves for induction of the pathogenic phase (16). The crude broth was then added to the assay mixture containing yeast CP. After an incubation period of only 10 minutes, ^{13}C labeled peptide substrate was added. NMR analysis of the digestion showed complete suppression of product formation, thus demonstrating the presence of proteasome inhibiting substances. Despite the high chemical heterogeneity covering all types of biomolecules present in culture broth, the signal to noise ratio in the decisive spectral range from 173 to 177 ppm was unaffected by interference. Confirming the univocal results gained by our novel method, SylA was purified from the respective culture broth and analyzed by HPLC as described (16).

Identification of candidate organisms for analysis. Next, we aimed to identify other organisms producing inhibitors against the CP. SylA is produced *in vivo* by a non-ribosomal peptide synthethase, which is constituted by an array of enzymes responsible for attachment of amino acid building blocks and introduction of chemical modifications. SylD, a 460 kDa multidomain enzyme, represents the major part of this assembly line and was chosen for BLAST alignment (17, 18). The search yielded hits among various *Photorhabdus* and *Burkholderia* species, which can therefore be suggested to produce analogous natural products. This group also comprises *Burkholderia pseudomallei*, the causative agent of melioidosis (19). Intriguingly, the related but less human pathogenic bacterium *Burkholderia mallei*, carries an analogous gene cluster, which is inactivated by transposon-mediated rearrangement, hence suggesting a significant contribution to virulence of the respective proteasome inhibiting compound (17). From this group of organisms, we chose the insect parasite bacterium *Photorhabdus luminescens*, as this S1 pathogen can be handled easily. The organism secretes intensely red-colored compounds (20, 21) not suitable for analysis with common assay types, hence representing a perfect candidate for a proof of concept of our detection method.

Induction of the pathogenic phase in *P. luminescens*. *Photorhabdus* was grown in SRM_{AF} medium containing the phenolic sugar arbutin present in leaves, which induces secretion of the SylA virulence factor from the plant pathogen *P. syringae* (22). However, no inhibitor production was detected by using our NMR assay, thus implying a divergent evolution of the sensory system of both species to adapt to their respective host organisms. *P. luminescens* obviously requires a different molecular trigger present in insects to start its pathogenic phase. Screening of diverse growth media with our NMR-based methodology revealed that an osmotic shock is necessary to mimic the environmental changes upon intrusion into the insect body and in turn to initiate inhibitor secretion (Supplementary Information). Proteolytic

processing of the substrate peptide was completely precluded under these conditions, indicating the presence of at least one highly potent CP inhibitor.

Isolation and structure elucidation of the inhibitors. To identify the CP inhibiting compounds from *Photorhabdus*, we have established an isolation procedure from liquid broth (see Online Methods). Intriguingly, from 3 L culture broth we received two CP inhibitors with a final yield of 10 mg each exhibiting molecular masses of 520 and 534 $g \cdot mol^{-1}$. Comparison of the LC-MS profile with a *Photorhabdus* culture exclusively grown at high salt condition revealed that the spectrum of secondary metabolites changed dramatically, thus reflecting a complete switch of life stages including the production of proteasome inhibitors (Supplementary information Fig. S1).

Structure elucidation of the two compounds by 2D-NMR analysis resulted in the molecules glidobactin A (GlbA), which had been known to be the strongest proteasome inhibitor identified so far (23, 24), as well as a molecule that has been named cepafungin I (CepI) in literature (25) (Fig. 2A). Despite the high similarity of the isolated molecules, CepI has never been investigated with respect to its properties as a proteasome inhibitor. Both CepI and GlbA share a 12 membered macrolactam ring system that is linked to a fatty acid tail. As the only difference, this apolar chain is terminally branched and carries an additional methyl moiety in the case of CepI, whereas it is linear in GlbA.

***In vitro* functional and structural characterization of GlbA and CepI.** Investigating the inhibitory potential of both compounds, we performed IC_{50} measurements with yeast CP using the established NMR assay for the ChTL activities. Remarkably, the IC_{50}-value for CepI (4 nM) was five times lower compared to GlbA (19 nM, Fig.2C). Evaluation of the stoichiometry between CepI and CP reveals that 100% inhibition is already observed at a ratio of 2:1, thus reaching the detection limit of the assay with regard to the two-fold symmetry of the proteasomal subunits. These results could be verified by established fluorescence based

assays, as the isolated compounds were uncolored and therefore did not cause quenching effects compared to the crude culture broth. Moreover, the high consistency between the data gained from both recording techniques confirms the equivalence of the NMR approach, using a natural and active-site specific proteasome substrate, in contrast to common assay types. In addition, measurements were expanded on evaluation of the TL and CL sites. The TL activity was inhibited to 24 nM for CepI and 193 nM for GlbA, respectively, thus exhibiting the same tendency as observed for the β5 subunit (Fig. S2). The proteasomal CL activity was not affected by either compound up to concentrations as high as 100 µM. These results were surprising since only a minor change such as a methyl group at the distal end from the active proteasomal Thr-1O$^{\gamma}$ residue has such an impact on the binding affinity.

Therefore, we performed crystal structure analysis of CepI and GlbA in complex with the yeast CP at 2.6 Å (R_{free}=24.3%) and 3.0 Å (R_{free}=22.7%) resolution for characterizing both inhibitors at the molecular level (Supplementary Information). Electron densities display covalent and irreversible binding of Thr-1O$^{\gamma}$ to the macrolactam ring via ether bond formation, which was confirmed by a gel shift assay (Fig. 2D-E). Intriguingly, the aliphatic fatty acid chains of GlbA and CepI point towards a hydrophobic patch formed by subunit β6 adjacent to the catalytically active β5 subunit. However, in contrast to the linear aliphatic chain of GlbA, the branched isopropyl side chain of CepI is further stabilized in a lipophilic pocket by strong van-der-Waals interactions (Fig. 2E-G). In conclusion, structural evaluation of SylA, GlbA and CepI suggests a directed evolution: starting from a charged and highly polar moiety adjacent to the macrolactam scaffold with impaired binding affinity, continuing with enhanced decoration as well as exploitation of the distant hydrophobic pocket in GlbA by an aliphatic linker and eventually yielding an optimized solution with maximum inhibition values for CepI. Analysis of the other active proteasomal subunits reveals that the β2 active site is occupied, whereas β1 was found empty, hereby confirming the *in vitro* results.

Equivalently to β5, the enhanced inhibitory strength of CepI versus GlbA against the TL activity can be explained by apolar interactions with a distal lipophilic patch via its branched fatty acid tail.

Cell culture experiments. In order to investigate cytotoxic effects on HeLa cancer cells upon treatment with GlbA/CepI, we determined the time-dependent viability at a final compound concentration of 1 μM (Fig. 3A). Both compounds, GlbA and CepI, exhibit significantly increased cytotoxicity versus the standard proteasome inhibitor MG132, an artificial and cell penetrating aldehyde peptide (27). This finding is also in agreement with their superior binding strength over MG132, which features an IC_{50} value of 270 nM against the ChTL activity *in vitro*. Although it has been shown that inhibition of β5 alone is sufficient for cytotoxicity of a compound, it is considerably increased if also a second subunit is affected (28). This furthermore explains the enhanced effects of the syrbactin compounds, which bind both to the β5 and the β2 subunits. Comparison between CepI and GlbA reveals that cancer cells treated with CepI displayed increased lethality than in the case of GlbA, again reflecting the results received by the *in vitro* experiments.

Assessing intracellular proteasome inhibition upon treatment with both natural compounds, we analyzed degradation of the natural proteasome substrate IκB. In most human cells, the nuclear NF-κB transcription factor is inactively sequestered in the cytosol by the inhibitory IκB protein, whose ubiquitin mediated degradation is initiated by the inflammatory cytokine IL-1 (29). By incubation with GlbA or CepI before addition of IL-1, however, the digestion of IκB is prevented, hence demonstrating the cell penetration and intracellular proteasome inhibition by the natural compounds (Fig. 3B).

Discussion

The results gained by our experiments are promising and make CepI a candidate for further drug development. Being the most powerful proteasome inhibitor described to date, its secretion is strictly controlled in *Photorhabdus* (Supplementary information). The bacterium, which lives in the gut of the nematode *Heterorhabditis*, presumably suspends production of GlbA and CepI until it is released into the hemocoel of an insect larva, whereupon they kill their mutual prey in a concerted action to reproduce new bacteria and nematodes (30). Hence, GlbA and CepI are proteasome inhibitors to which a biological function could be assigned. Despite the rigid environmental regulation, the discovery of the two natural compounds from *Photorhabdus* was feasible due to the novel approach established in this work. The determination of the appropriate stimuli for pathogenic organisms to enter the virulent life-stages, when most secondary metabolites are produced, is of crucial importance, as the majority of all genes involved in production of natural compounds are usually found silent under common growth conditions. As many other organisms, like the human pathogen *Burkholderia pseudomallei*, carry gene clusters for putative proteasome inhibitors, the application of the developed methodology for screening of such triggers will identify promising new natural products, which may lead to the development of new drugs for treatment of various diseases. Eventually, we anticipate that a transfer of the established screening procedure to other targets of pharmaceutical interest will facilitate the identification of natural inhibitory compounds for these enzymes.

Materials and Methods

NMR proteasome assay. Purification of the 20S proteasome from *S. cerevisiae* was performed as described previously (3). The assay mixture containing 10 µg/ml yeast CP, 100 mM Tris (pH 8.0), 0.01% SDS and 300 µl sterile filtrated culture broth was incubated for 10

minutes at RT. Labeled peptide was added to a final concentration of 2 mM and incubated for 6 hours. The assay was quenched by ultrafiltration, completed with D_2O and recorded in a 500 MHz spectrometer (Bruker Topspin ^{13}C-Cryo NMR). IC_{50} measurements were carried out accordingly with the purified compounds dissolved in DMSO. Remaining activity was calculated by scaling the ratio of the product to the educt peak and compared with a blank sample.

Secretion and Purification of GlbA/CepI. A preculture of *P. luminescens ssp. laumondii* (DSM No 15139) was grown at high osmolarity (0.2% Tryptone, 0.5% Yeast Extract, 1% NaCl) for three days at 28 °C, which was then used to inoculate medium without NaCl in a 1/100 ratio. During further incubation for three days, a hydrophobic resin (XAD-16) was added to the culture broth, which was afterwards extracted with methanol. The extract was subjected to a silica column, which was washed with cyclohexane and eluted with ethyl acetate. Fractions containing inhibitors were identified by the proteasome assay and applied to RP-C18 HPLC chromatography. GlbA and CepI eluted at approximately 55% acetonitrile in a 10-70% gradient over 1 h on a 250/10 mm column.

Cell culture assay. Viability measurements with HeLa cells were performed at a final inhibitor concentration of 1 µM at 6, 10, 24 and 48 hours by Alamar Blue assays as described previously (31); MG132 was purchased from Bachem. For Western blot analysis of IκB accumulation, HeLa cells were incubated with 40 µM inhibitors for 6 hours and then stimulated by addition of IL-1 at a concentration of 30 ng/ml for 20 minutes before harvesting. After cell lysis, 10 µg protein was applied to 15% SDS-PAGE. Western blot analysis of IκB was standardized by comparison to the GADPH housekeeping protein.

Acknowledgements

We thank Richard Feicht for yeast proteasome purification as well as Nerea Gallastegui, Haissi Cui and Achim Krüger for assistance in cell culture assays. Katja Bäuml is acknowledged for help with peptide synthesis. We are grateful to the staff of the Beamlines X06SA and X06DA at the Paul Scherrer Institute, SLS, Villingen, Switzerland for their support during data collection. M. K. was funded by an ERC starting grant (grant No. 258413).

Author contributions

M.G. designed experiments. C.B. designed and synthesized the peptide substrate; R.D. provided *P.syringae* strains and conditioned media. Isolation of natural products and structure elucidation was performed by M.S. and P.B. Activity tests, crystallographic experiments and cell culture assays were conducted by M.S.; M.G. and M.S. collected and analyzed crystallographic data. M.K. contributed to the interpretation of the received results. M.G. and M.S. wrote the manuscript.

Author information

The authors declare no conflict of interest.

Data deposition: The atomic coordinates and structure factors have been deposited in the Protein Data Bank, www.pdb.org [PDB ID codes 4FZC (CP:CepI) and 4FZG (CP:GlbA)].

Correspondence and requests for materials should be addressed to M.G. (michael.groll@ch.tum.de).

References

1. Hershko A, Ciechanover A (1998) The ubiquitin system. *Annu Rev Biochem* 67:425-479.
2. Gallastegui N, Groll M (2010) The 26S proteasome: assembly and function of a destructive machine. *Trends Biochem Sci* 35(11):634-642.
3. Groll M, *et al.* (1997) Structure of 20S proteasome from yeast at 2.4 A resolution. *Nature* 386(6624):463-471.
4. Huber EM, *et al.* (2012) Immuno- and constitutive proteasome crystal structures reveal differences in substrate and inhibitor specificity. *Cell* 148(4):727-738.
5. Unno M, *et al.* (2002) Structure determination of the constitutive 20S proteasome from bovine liver at 2.75 A resolution. *J Biochem* 131(2):171-173.
6. Orlowski M (1990) The multicatalytic proteinase complex, a major extralysosomal proteolytic system. *Biochemistry* 29(45):10289-10297.
7. Huber EM, Groll M (2012) Inhibitors for the immuno- and constitutive proteasome: current and future trends in drug development. *Angew Chem Int Ed* 51(35):8708-8720.
8. Richardson PG, Hideshima T, Anderson KC (2003) Bortezomib (PS-341): a novel, first-in-class proteasome inhibitor for the treatment of multiple myeloma and other cancers. *Cancer Control* 10(5):361-369.
9. Arastu-Kapur S, *et al.* (2011) Nonproteasomal targets of the proteasome inhibitors bortezomib and carfilzomib: a link to clinical adverse events. *Clin Cancer Res* 17(9):2734-2743.
10. Gräwert M, Groll M (2012) Exploiting nature's rich source of proteasome inhibitors as starting points in drug development. *Chem Commun* 48(10):1364-1378.
11. Khan M, Stewart AK (2011) Carfilzomib: a novel second-generation proteasome inhibitor. *Future Oncol* 7(5):607-612.
12. Meng L, *et al.* (1999) Epoxomicin, a potent and selective proteasome inhibitor, exhibits in vivo antiinflammatory activity. *Proc Natl Acad Sci U S A* 96(18):10403-10408.
13. Groll M, Kim K, Kairies N, Huber R, Crews C (2010) Crystal structure of epoxomicin:20S proteasome reveals molecular basis for selectivity of α'β'-epoxyketone proteasome inhibitors. *J Am Chem Soc*, pp 1237-1238.
14. Dick TP, *et al.* (1998) Contribution of proteasomal beta-subunits to the cleavage of peptide substrates analyzed with yeast mutants. *J Biol Chem* 273(40):25637-25646.
15. Adams J, *et al.* (1998) Potent and selective inhibitors of the proteasome: dipeptidyl boronic acids. *Bioorg Med Chem Lett* 8(4):333-338.
16. Wäspi U, Blanc D, Winkler T, Rüedi P, Dudler R (1998) Syringolin, a Novel Peptide Elicitor from *Pseudomonas syringae pv. syringae* that Induces Resistance to *Pyricularia oryzae* in Rice. Molecular Plant-Microbe Interactions, pp 727-733.
17. Schellenberg B, Bigler L, Dudler R (2007) Identification of genes involved in the biosynthesis of the cytotoxic compound glidobactin from a soil bacterium. *Environ Microbiol* 9(7):1640-1650.
18. Krahn D, Ottmann C, Kaiser M (2011) The chemistry and biology of syringolins, glidobactins and cepafungins (syrbactins). *Nat Prod Rep* 28(11):1854-1867.
19. Wiersinga WJ, van der Poll T, White NJ, Day NP, Peacock SJ (2006) Melioidosis: insights into the pathogenicity of *Burkholderia pseudomallei*. *Nat Rev Microbiol* 4(4):272-282.

20. Frackman S, Anhalt M, Nealson KH (1990) Cloning, organization, and expression of the bioluminescence genes of *Xenorhabdus luminescens*. *J Bacteriol* 172(10):5767-5773.
21. Brachmann AO, *et al.* (2012) Triggering the production of the cryptic blue pigment indigoidine from *Photorhabdus luminescens*. *J Biotechnol* 157(1):96-99.
22. Waspi U, Blanc D, Winkler T, Ruedi P, Dudler R (1998) Syringolin, a novel peptide elicitor from *Pseudomonas syringae pv. syringae* that induces resistance to *Pyricularia oryzae* in rice. *Molecular Plant-Microbe Interactions* 11(8):727-733.
23. Groll M, *et al.* (2008) A plant pathogen virulence factor inhibits the eukaryotic proteasome by a novel mechanism. *Nature* 452(7188):755-758.
24. Oka M, *et al.* (1988) Glidobactins A, B and C, new antitumor antibiotics. I. Production, isolation, chemical properties and biological activity. *J Antibiot* 41(10):1331-1337.
25. Shoji J, *et al.* (1990) Isolation of cepafungins I, II and III from *Pseudomonas* species. *J Antibiot* 43(7):783-787.
26. Loewe J, *et al.* (1995) Crystal Structure of the 20S Proteasome from the Archaeon *T. acidophilum* at 3.4 A Resolution. *Science* 268(5210):533-539.
27. Bush KT, Goldberg AL, Nigam SK (1997) Proteasome inhibition leads to a heat-shock response, induction of endoplasmic reticulum chaperones, and thermotolerance. *J Biol Chem* 272(14):9086-9092.
28. Screen M, *et al.* (2010) Nature of pharmacophore influences active site specificity of proteasome inhibitors. *J Biol Chem* 285(51):40125-40134.
29. Ortis F, *et al.* (2012) Differential usage of NF-κB activating signals by IL-1β and TNF-α in pancreatic beta cells. *FEBS Lett* 586(7):984-989.
30. Waterfield NR, Ciche T, Clarke D (2009) *Photorhabdus* and a host of hosts. *Annu Rev Microbiol* 63:557-574.
31. Macherla V, *et al.* (2005) Structure-activity relationship studies of salinosporamide A (NPI-0052), a novel marine derived proteasome inhibitor. *J Med Chem* 48(11):3684-3687.

Figure Legends

Fig. 1. NMR peptide assay. (A) Primary sequence of the substrate with the scissile peptide bond and the ^{13}C label. (B) NMR spectrum of substrate digestions with the uncleaved educt and the carboxylic acid product at 173 and 177 ppm, respectively (upper panel). Product peak formation is suppressed upon addition of a CP inhibiting culture broth (lower panel).

Fig. 2. *In vitro* functional and structural characterization of GlbA and CepI. (A) NMR deduced structures of GlbA/CepI with the proteasome binding sites S1 and S3 as well as the hydrophobic patch S_L. (B) SylA, featuring a hydrophilic carboxylic acid tail. (C) IC_{50} curves for the ChTL activity measured for GlbA (green) and CepI (blue) with ^{13}C labeled peptide

substrate; black curves depict equivalent measurements with the fluorogenic Suc-Leu-Leu-Val-Tyr-AMC substrate (error bars are too small to be visible) . (D) Western blot on a β5-$(His)_6$ yeast CP mutant +/- treatment with CepI. The gel shift indicates an increased molecular mass by covalent and irreversible binding. (E) Structural superposition of GlbA and CepI bound to yeast CP; the differing methyl moiety is indicated by a red arrow. (F) Surface representation of CepI in the β5 substrate binding channel. Colors indicate positive and negative electrostatic potentials contoured from -30 kT/e (bright red) to +30 kT/e (bright blue) (G) Stereoview of the $2F_o$ - F_c omit electron density map (grey mesh, 1σ) for the β5 active site. Hydrogen bonds are indicated by dashed lines, whereas the arrow pronounces the accurate fitting of the P1 methyl side chain of the inhitibor. The lipophilic pocket of the S_L site is formed by Tyr-5, Pro94, Tyr96 and Pro115 from β6 (amino acid numbering according to Löwe et al. (26).

Fig. 3. Cell culture assays. (A) Cytotoxicity is measured by performing the Alamar Blue assay with HeLa cells after 6, 10, 24 and 48 h for MG132 (black), GlbA (green) and CepI (blue) at 1 µM concentration. (B) Western blot on IκB +/- IL-1 induction in HeLa cells, which were treated for 6 hours with 50 µM of MG132, GlbA, CepI or DMSO. Proteasomal IκB degradation is initiated by IL-1 signaling, whereas it is prevented after addition of the cell penetrating CP inhibitors. The GADPH housekeeping protein was co-stained for quantification.

Online Methods

Peptide synthesis. The ^{13}C-labeled CP substrate peptide was synthesized at a 0.2 mmol scale on a custom-modified Applied Biosystems 433A peptide synthesizer using S-DVB (stryrene-divinylbenzene) resin carrying an -OCH_2-PAM (Applied Biosystems, Foster City, CA) and a thioester-generating linker following an *in-situ* neutralization protocol for machine-assisted Boc (tert.-butoxycarbonyl) chemistry (32, 33). Side chain protecting groups were: Arg(Tos), Asn(Xan), Glu(OcHx), Ser(Bzl) and Tyr(2BrZ). Boc-Phe(Cα-^{13}C) was obtained from euriso-top. The peptide was released from resin by treatment with liquid HF for 1 hour at 0 °C in the presence of 5% (v/v) *p*-cresol. 10 ml of liquid HF were used for 1 g of peptide-resin. Purification of the crude peptide was achieved using a semipreparative RP-HPLC C4-column (Grace, Lokeren, Belgium) and a gradient of 40 to 65% buffer B (acetonitrile + 0.08% TFA) in buffer A (water + 0.1% TFA) over 60 minutes. Product containing fractions were identified by ESI-MS (electrospray ionization mass spectrometry) and pooled accordingly. 24% of purified peptide was obtained from crude material and dissolved in DMSO for application in digestion assays.

Secretion and Purification of GlbA/CepI. Bacteria were grown in TYEA medium (0.2% Bacto-Tryptone, 0.5% Yeast Extract, 1% NaCl per litre) for 3 days at 28 °C. This culture was used to inoculate TYEB medium (TYEA without NaCl) at a ratio of 1/100. Solid adsorber resin (XAD-16) was added to the culture broth, which was in turn incubated for three days. The resin was filtrated and extracted with methanol. After concentrating the sample by evaporation, it was applied to a silica column (Silica Gel 60 by Merck). The column was washed with cyclohexane and eluted with ethylacetate. All fractions were tested by the NMR proteasome assay and positive fractions were applied to preparative HPLC chromatography (RP-C18, 150 mm, 1 cm id, 3.5 µm) with a gradient of 10-70% acetonitrile within 60 minutes. Fractions were again tested by the NMR assay; GlbA and CepI eluted at approximately 55%

acetonitrile. Mass spectrometrical analysis was perfomed by ESI-MS (Thermo-Fisher-Scientific Orbitrap). NMR measurements for structure elucidation were carried out in D_6-DMSO at 500 MHz with respective compound concentrations of 25 mM.

IC_{50} measurements by fluorogenic substrates. *In vitro* proteasome inhibition assays were performed in 96-well microtiter plates with 10 µg/ml yeast CP in 100 mM Tris (pH 8.0) supplemented with 0.01% SDS. Inhibitors were added in DMSO at various concentrations with three repetitions each. After a reaction time of 30 minutes, the fluorogenic substrates Suc-Leu-Leu-Val-Tyr-AMC, Z-Ala-Arg-Arg-AMC or Z-Leu-Leu-Glu-AMC were added for analysis of ChTL, TL the CL activities, respectively. The assay mixture was incubated for further 60 minutes; fluorescence and excitation were monitored with a Varian Cary Eclipse Photofluorometer at 460 nm and 360 nm, respectively,

Gel shift assay. A tagged β5-$(His)_6$ yeast proteasome mutant was incubated at a concentration of 1 mg/ml with inhibitor or DMSO in 100 mM Tris pH 8.0 for one hour and applied to a 12% SDS-PAGE. The β5-$(His)_6$ subunit was stained by Western blot analysis. Covalent and irreversible modification of the subunit is accompanied by a gel shift, whereas non-covalent or reversible inhibitors detach during electrophoresis.

Cocrystallisation and structure elucidation. Crystals of the yeast CP were grown in hanging drops at 24 °C as described (34). The protein concentration used for crystallisation was 40 mg/ml in Tris-HCl (10 mM, pH 7.5) and EDTA (1 mM). The drops contained 3 µl of protein and 2 µl of the reservoir solution (30 mM magnesium acetate, 100 mM morpholino-ethane-sulphonic acid (pH 7.2) and 10% 2-methyl-2,4-pentanediol). Crystals were incubated at 2 mM inhibitor concentration for 24 hours, followed by soaking in a cryoprotecting buffer (30% MPD, 20 mM magnesium acetate, 100 mM morpholino-ethane-sulfonic acid pH 6.9) and super-cooled in a stream of liquid nitrogen gas at 100 K (Oxford Cryo Systems).

Data of the CP:CepI and the CP:GlbA complexes were collected to 2.8 and 3.0 Å, respectively, using synchrotron radiation (λ = 1.0 Å) at the X06SA-beamline (SLS/Villingen/Switzerland). The space group belongs to $P2_1$ with cell dimensions of a=134 Å, b=301 Å, c=144 Å and β =112° (see Supplementary Table S3). X-ray intensities were evaluated by using XDS (35) and data reduction was performed with XSCALE (35). The anisotropy of diffraction was corrected by an overall anisotropic temperature factor by comparing observed and calculated structure amplitudes using the program CNS (36). Electron density was improved by averaging and back transforming the reflections 10 times over the twofold non-crystallographic symmetry axis using the program package MAIN (37). Conventional crystallographic rigid body, positional and temperature factor refinements were carried out with CNS using the yeast 20S CP structure as starting model (PDB accession code 1RYP) (3). Model building was performed with the program MAIN (37). Apart from the bound inhibitor molecules, structural changes were only noted in the specificity pockets. Temperature factor refinement indicates full occupancies of all inhibitor binding sites.

32. Camarero JA, Muir TW (1999) Chemical Ligation of Polypeptides. *Current Protocols in Protein Science*, pp 18.14.11-18.14.21.
33. Schnölzer M, Alewood P, Jones A, Alewood D, Kent SB (1992) In situ neutralization in Boc-chemistry solid phase peptide synthesis. Rapid, high yield assembly of difficult sequences. *Int J Pept Protein Res* 40 (3-4):180-193.
34. Groll M & Huber R (2005) Purification, crystallization, and X-ray analysis of the yeast 20S proteasome. *Methods Enzymol* 398:329-336.
35. Kabsch W (2010) XDS. *Acta Crystallogr D Biol Crystallogr* 66 (Pt 2):125-132.
36. Brünger AT, *et al.* (1998) Crystallography & NMR system: A new software suite for macromolecular structure determination. *Acta Crystallogr D Biol Crystallogr* 54 (Pt 5):905-921.
37. Turk D (1992) Improvement of a programm for molecular graphics and manipulation of electron densities and its application for protein structure determination. Thesis Technische Universitaet Muenchen.

Supplementary Information for

One-shot analysis of microbial secretions identifies highly potent proteasome inhibitor

Martin Stein, Philipp Beck, Markus Kaiser, Robert Dudler, Christian F. W. Becker and Michael Groll*

*Correspondence to michael.groll@ch.tum.de

Analysis of peptide cleavage pattern and specificity. The peptide cleavage site was determined by LC-MS analysis of the digestion products in an *in vitro* assay containing 10 µg/ml yeast CP, 100 mM Tris (pH 8.0), 0.01% SDS, 10% DMSO and 2 mM peptide, which was incubated for 6 hours at 37 °C. Confirming the specificity of the probe molecule towards the β5 subunit, hydrolysis was prevented in the same assay after addition of the synthetic boronic acid inhibitor MG262 (Enzo Life Sciences), which exhibits inhibition merely of the ChTL activity.

Induction of biosynthesis of GlbA and CepI in *P. luminescens*. Initially, an NMR screen of *Photorhabdus* cultures was carried out to detect suitable growth conditions for inhibitor secretion. However, application of standard media and variation of their respective composition, as well as complementation with various additives, failed to initiate the pathogenic phase in *Photorhabdus*. Furthermore, mimicking previously described conditions for producing SylA and GlbA from *P. syringae* and *Burkholderiales* strain K481-B101 did not yield any positive result. We therefore performed inoculation experiments by transmission of precultured *Photorhabdus* bacteria to differently conditioned media to analyze the effects of environmental shifts. An abrupt change of osmolarity, going from 170 mM to 0 mM NaCl, resulted in complete inhibition of the proteasome in our NMR assay, thus identifying the conditions to trigger the virulent phase. In agreement to previous findings (1, 2), we could demonstrate that there is no consensus between the different molecular stimuli among the organisms producing SylA related compounds. To further confirm the quality of our NMR based assay we performed LC-MS runs of *Photorhabdus* cultures with or without submission to an osmotic shock and could show that under common growth conditions none of the inhibitors is detectable (Figure S1). In conclusion, our data indicate that secretion of GlbA and CepI is limited to a well-defined environmental shift, reflecting the distinct life-stages of *Photorhabdus*.

Table S1. Screening of different media and additives.

Standard media: LB, 2xTY, CY, SRM, TYEA, PDB, DSMZ media 1, 54, 220	
Changed parameters in these media:	Sugar, Casitone, Peptone, yeast extract and salt ingredients
Additives:	Fructose, maltose, arbutin, sucrose and lactose
	L-proline, L-arginine
	Iron(III)chloride, iron(II)chloride, soluble and insoluble magnesium and calciumsalts
Other parameters:	Temperature (18 to 34 °C in steps of 2 °C), rotation speed, incubation time (one to ten days), inocculation density

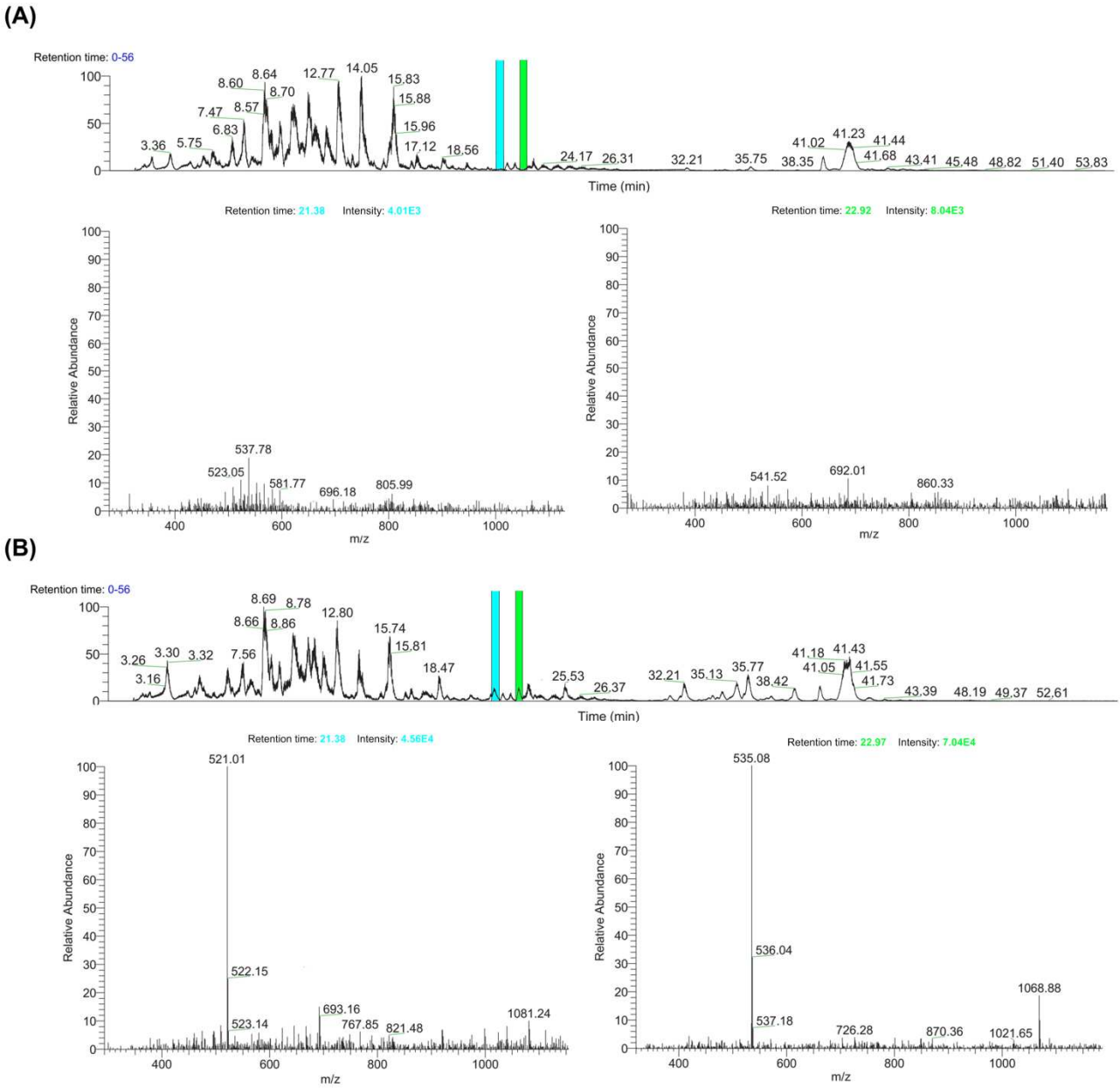

Figure S1: Comparison between GlbA and CepI secretion in standard medium and after osmotic shock. LC-MS runs of saturated *Photorhabdus* cultures grown in 2xTY (A) or TYEA/TYEB induction media (B). In agreement to our NMR results, both samples display significant differences in the elution interval between 20 and 40 minutes. The proteasome inhibitors GlbA (21.38 minutes, blue bar) and CepI (22.92 minutes, green bar) were only detected in the culture treated with TYEB (B).

Purification of GlbA and CepI from *P. luminescens* secretions. Secretions and extracts of microorganisms are often colored, making UV-Vis based assay techniques prone to color quenching artifacts. *Photorhabdus* produces a whole range of colored substances (Figure S2).

Figure S2: Colored culture broth of *P. luminescens*. The culture broth has a dark shade of red (left), rendering UV-Vis based techniques impossible. Chromatographic separation on a silica column (right) reveals that a whole array of colored substances is produced by *Photorhabdus*.

IC_{50} measurements of the CL and TL activities. Just as in the case of the ChTL activity, inhibition of the β2 subunit is enhanced for CepI (Fig. S3), thus reflecting increased hydrophobic interactions between its aliphatic fatty acid chain and the adjacent β3 subunit. In contrast, neither of the compounds binds to β1, which is again in agreement with the *in vitro* assay results.

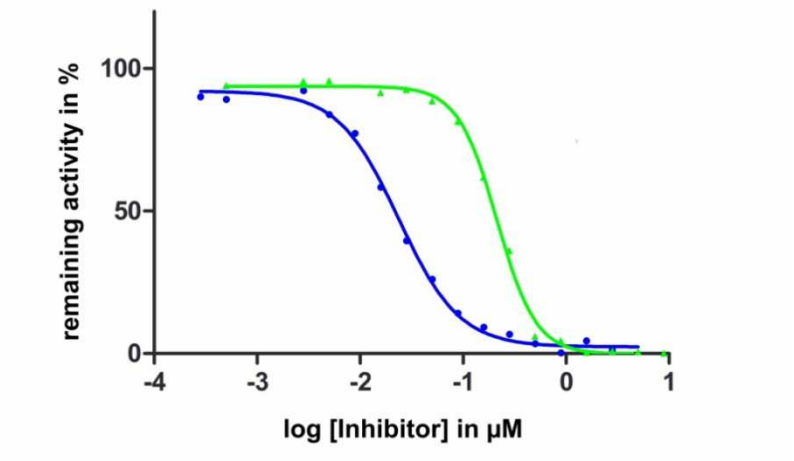

Figure S3: Inhibition of the TL activity. The IC_{50} value of CepI (blue curve) is six times decreased compared to GlbA (green).

NMR structure elucidation of GlbA and CepI. NMR peak assignments are listed in table S2 and refer to the atom numbering in figure S4. All spectra were recorded at 500 MHz in D_6-DMSO.

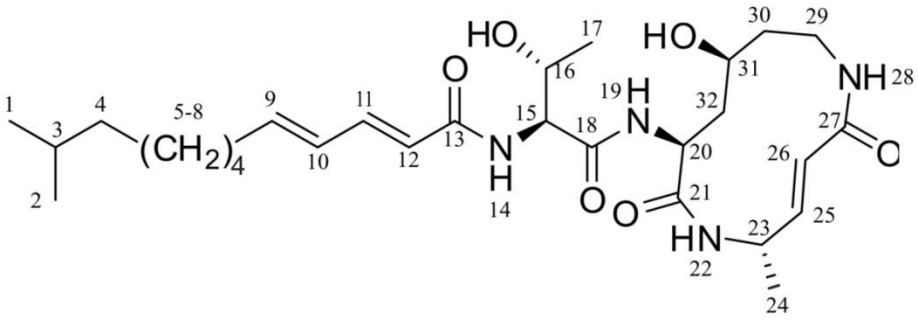

Figure S4: Molecular Structure of CepI with atom labelling

Table S2. NMR Spectroscopic data (D_6-DMSO) for CepI (a) and GlbA (b)

	δ_H, mult. (J [Hz])	δ_C	Type	COSY	HMBC
1a, 2a	0.84, d, (3.25)	23.03	CH_3	3a	1a, 2a, 3a, 4a
3a	1.50, m	27.82	CH	1a, 2a, 4a	1a, 2a, 4,a 5a
4a	1.15, m	38.86	CH_2	3a, 5a	1a, 2a, 3a, 5a, 6a
1b	0.86, t (7.0)	14.46	CH_3	3	3b, 4b
3b	1.26, m	31.68	CH_2	1b	1b
4b	1.26, m	26.21	CH_2		
5	1.26, m	27.08	CH_2	4a	
6	1.26, m	29.21	CH_2		

7	1.39, m	28.81	CH_2	8	5, 6, 8
8	2.13, m	32.76	CH_2	7, 9	7, 9, 10
9	6.11, m	142.68	CH	8, 10	7, 8, 10, 11
10	6.19, m	129.49	CH	9, 11	8, 9, 11
11	7.00, dd (15.0, 10.0)	140.24	CH	10, 12	9, 10, 12, 13
12	6.13, m	123.49	CH	11	11, 13
13	-	165.88	C(O)		11, 12
14	7.91, d (9.0)	-	NH	15	13, 15
15	4.29, m	58.49	CH	14, 16	16, 17, 18
16	3.97, m	67.18	CH	15, 17	
17	1.0, d (10)	20.46	CH_3	16	15, 16
18	-	169.86	C(O)		15, 19
19	7.76, d (7.0)	-	NH	20	18, 20, 21
20	4.34, m	51.66	CH	19, 32	
21	-	171.44	C(O)		19
22	8.69	-	NH	23	
23	4.37, m	45.21	CH	22, 24, 25	
24	1.22, m	19.05	CH_3	23	23
25	6.41, d (15.0)	143.56	CH	26	
26	6.19, m	140.23	CH	25	26
27	-	168.09	C(O)		25, 29
28	7.44, t (5.5)	-	NH	29	26, 29, 30
29	3.02, m	40.40	CH_2	28, 30	27, 28, 30
30	1.45, m	40.07	CH_2	29, 31	29
31	3.58, m	67.57	CH	30, 32	30
32	1.85, m 1.58, d (11.5)	42.93	CH_2	31, 32, 20	

Crystallographic data. Despite the existing structural information of the CP:GlbA complex (PDB code 3BDM), we performed crystal structure analysis also with the isolated natural compound from *Photorhabdus* for direct comparison, as the crystallization conditions were slightly modified.

Table S3. Data collection and refinement statistics.

	CP:CepI [a]	CP:GlbA [a]
Crystal parameters		
Space group	$P2_1$	$P2_1$
Cell constants (Å) / °	a=135,7	134.8
(dataset was collected from	b=301,0	300.4
1 crystal / 1 CP per AU)	c=144,8	144.5

	β=112,9	112.7
Data collection		
Beamline	X06SA, SLS	
Wavelength (Å)	1.0	
Resolution range (Å) [b]	25-2.8	15-3.0
No. observations	837332	724190
No. unique reflections [c]	256455	209581
Completeness (%) [b]	97,8 (99,0)	99.3 (99.7)
R_{merge} [b, d]	7,7 (61,4)	6.7 (47.2)
I/σ (I) [b]	13,0 (2,4)	15.2(3.2)
Refinement (CNS)		
Resoltution range (Å)	15-2,8	15-3.0
No. refl. working set	242408	197883
No. refl. test set	12718	10363
No. non hydrogen	49548	49548
No. of ligand atoms	140	136
Water	1320	1290
R_{work}/R_{free} (%) [e]	21.3 / 24.3	19.8 / 22.7
rmsd bond (Å) / (°) [f]	0.007 / 1.32	0.007 / 1.32
Ramachandran Plot (%) [g]	95.0 / 4.7 / 0.3	94.7 / 4.8 / 0.5

[a] Dataset has been collected on a single crystal

[b] The values in parentheses of resolution range, completeness, R_{merge} and I/σ (I) correspond to the last resolution shell

[c] Friedel pairs were treated as identical reflections

[d] $R_{merge}(I) = \Sigma_{hkl}\Sigma_j |[I(hkl)_j - I(hkl)]| / \Sigma_{hkl} I_{hkl}$, where $I(hkl)_j$ is the measurement of the intensity of reflection hkl and $\langle I(hkl) \rangle$ is the average intensity

[e] $R = \Sigma_{hkl} | |F_{obs}| - |F_{calc}| | / \Sigma_{hkl} |F_{obs}|$, where R_{free} is calculated without a sigma cut off for a randomly chosen 5% of reflections, which were not used for structure refinement, and R_{work} is calculated for the remaining reflections

[f] Deviations from ideal bond lengths/angles

[g] Number of residues in favoured region / allowed region / outlier region

1. Waspi U, Blanc D, Winkler T, Ruedi P, & Dudler R (1998) Syringolin, a novel peptide elicitor from *Pseudomonas syringae pv. syringae* that induces resistance to Pyricularia oryzae in rice. *Molecular Plant-Microbe Interactions* 11(8):727-733.
2. Oka M*, et al.* (1988) Glidobactins A, B and C, new antitumor antibiotics. I. Production, isolation, chemical properties and biological activity. *J Antibiot (Tokyo)* 41(10):1331-1337.